NEOPLASIA
www.neoplasia.com

Volume 20 Number 11 November 2018 pp. 1135–1143 1135

Inactivation of PRIM1 Function Sensitizes Cancer Cells to ATR and CHK1 Inhibitors[1]

Albert Job, Lisa-Maria Schmitt, Lisa von Wenserski[2], Brigitte Lankat-Buttgereit, Thomas M. Gress, Malte Buchholz and Eike Gallmeier

Center for Tumor Biology and Immunology, Department of Gastroenterology, Endocrinology and Metabolism, University Hospital of Marburg, Philipps-University Marburg, Marburg, Germany

Abstract

The phosphoinositide 3-kinase–related kinase ATR is a central regulator of the DNA damage response. Its chemical inhibition eliminates subsets of cancer cells in various tumor types. This effect is caused at least partly by the synthetically lethal relationship between *ATR* and certain DNA repair genes. In a previous screen using an siRNA library against DNA repair genes, we identified *PRIM1*, a part of the polymerase α-primase complex, as acting synthetically lethal with *ATR*. Applying a genetic *ATR* knock-in model of colorectal cancer cells, we confirmed that *PRIM1* depletion inhibited proliferation of *ATR*-deficient cells and excluded artifacts due to clonal variation using an *ATR* reexpressing cell clone. We expanded these data by demonstrating in different cell lines that also chemical inhibition of ATR or its main effector kinase CHK1 reduces proliferation upon depletion of *PRIM1*. Mechanistically, *PRIM1* depletion in *ATR*-deficient cells caused S-phase stasis in the absence of increased DNA damage followed by Wee1-mediated activation of caspase 8 and apoptosis. As *PRIM1* inactivation sensitizes cancer cells to ATR and CHK1 inhibitors, mutations in *PRIM1* or other components of the polymerase α-primase complex could represent novel targets for individualized tumor therapeutic approaches using ATR/CHK1 inhibitors, as has been previously demonstrated for *POLD1*, the catalytic subunit of polymerase δ.

Neoplasia (2018) 20, 1135–1143

Introduction

Synthetic lethality is defined as the interaction between two genes in which single mutations alone are not lethal but in combination are incompatible with cell survival. This mechanism could facilitate an individualized and targeted cancer therapy through pharmacological inhibition of proteins that interact synthetically lethal with tumor-specific gene mutations [1]. A prominent example is the treatment of patients harboring *BRCA1/2*-deficient cancers using PARP inhibitors [2,3]. ATR is a phosphoinositide 3-kinase–related kinase and acts as central regulator of the replication checkpoint during the DNA damage response [4]. Activated by the accumulation of single-stranded DNA at sites of replication stress or DNA damage, ATR initiates replication fork stabilization, cell cycle arrest, and DNA repair via homologous recombination [5,6]. ATR inhibitors are currently tested in clinical trials either as stand-alone therapy or in combination with DNA-damaging agents. However, the specific determinants of therapeutic response are not sufficiently defined, as only subsets of tumor cells appear to be effectively eliminated [7,8].

Abbreviations: 5-FU, 5-fluouracil; CRC, colorectal cancer; DSB, double-strand break; FBS, fetal bovine serum; ICL, interstrand-crosslinking; MMC, mitomycin C; MSI, microsatellite instability; NTC, non-transfected cells; PBS, phosphate buffered saline; pol, polymerase; RPMI 1640, Roswell Park Memorial Institute; TBS-T, TBS + 0.1% Tween 20.

Address all correspondence to: Prof. Dr. med. Eike Gallmeier, Department of Gastroenterology, Endocrinology and Metabolism, University Hospital of Marburg, Baldingerstraße, 35043, Marburg, Germany. E-mail: eike.gallmeier@med.uni-marburg.de

[1] Competing Interests: The authors declare that they have no competing interest.

[2] Present address: Department of Oncology and Hematology, University Medical Center Hamburg-Eppendorf, Hamburg, Germany.

Received 2 July 2018; Revised 29 August 2018; Accepted 31 August 2018

1476-5586
https://doi.org/10.1016/j.neo.2018.08.009

Due to the above function of ATR, this selectivity could at least in part be attributable to a synthetically lethal relationship between *ATR* and certain DNA repair genes. This hypothesis is supported by a systematic screening approach performed previously by us using an siRNA library targeting 288 DNA repair genes [9] in a well-defined *ATR* knock-in model [10].

In this screen, we identified six genes which may act synthetically lethal with *ATR*, including *PRIM1*. *PRIM1* encodes the catalytic subunit of primase of the polymerase (pol) α-primase complex, a major polymerase during replication, mediating the *de novo* and progressive synthesis of hybrid RNA-DNA primer as starting point for the replication of the leading and lagging strand [11,12]. However, the significance of this polα-primase complex as a potential target for cancer therapy remains enigmatic.

In the study presented here, we confirmed and characterized the synthetic lethal relationship between *ATR* and *PRIM1*. In addition, we investigated the underlying molecular mechanism through assessment of cell cycle progression, apoptosis, and DNA damage in *PRIM1*-depleted cells upon either genetic or chemical disruption of *ATR* function.

Material and Methods

Cell Lines and Culture Conditions

The human colorectal cancer (CRC) cell lines DLD-1, SW480, and RKO were purchased from the Leibniz Institut DSMZ (Braunschweig, Germany) or the American Type Culture Collection (LGC Standards, Wesel, Germany), respectively. The human pancreatic cancer cell line PaTu 8988t was kindly provided by Hans-Peter Elsässer (Philipps-University Marburg, Germany). $ATR^{s/s}$ cells were kindly provided by Fred Bunz (John Hopkins University, Baltimore, MD, USA) and have been characterized previously [7,10,13]. All cell lines and clones were maintained in Roswell Park Memorial Institute (RPMI 1640) medium supplemented with 10% fetal bovine serum (FBS) and incubated at 37°C and 5% CO_2.

Establishment of an ATR Reexpressing Cell Clone

$ATR^{s/s}$ cells were co-transfected with vectors pcDNA3-ATR WT (Addgene plasmid #31611, conferring neomycin resistance), kindly donated by Aziz Sancar [14], and pLKO-U6-Tet-on-shNT5E-965 (conferring puromycin resistance), kindly provided by Stephan A. Hahn (Laboratory of Molecular Oncology, University Bochum, Germany), in a ratio of 10:1, as $ATR^{s/s}$ cells already harbor a neomycin resistance [10]. After transfection, the cells were maintained in RPMI 1640 containing 1 µg/ml puromycin (InvivoGen, San Diego, CA). After 3 weeks of selection, single puromycin-resistant cell clones were seeded and grown in 96-well plates and consecutively screened by immunoblotting for high expression of ATR as compared to $ATR^{s/s}$ cells. The clone with the highest expression of ATR was chosen for consecutive experiments (termed ATR^{resc}).

Drugs

AZD6738 and VE-822 were purchased from MedKoo Biosciences (Morrisville, NC), MK-8776 and LY2603618 from Selleckchem (Munich, Germany), and mitomycin C (MMC) and 5-fluouracil (5-FU) from Sigma-Aldrich (Hamburg, Germany). Oxaliplatin was kindly donated from the cytostatic drug department of the University Hospital Marburg.

Transfection

Reverse transfection was used for transfection experiments. siRNA targeting *PRIM1* (AACCACAGATCAAATACTTCA) (QIAGEN, Hilden, Germany) at a final concentration of 10 nM was incubated with HiPerFect from QIAGEN in RPMI 1640 medium free of FBS for 20 minutes at room temperature and then added to freshly seeded cells.

Cell Proliferations Assays

Cell proliferation assays were performed over a broad range of concentrations covering 100% to 0% cell survival. Either 600-800 cells of DLD-1 $ATR^{+/+}$, $ATR^{s/s}$, and ATR^{resc} were plated and transfected for 144 hours in 96-well plates to reach a final confluence of 50%-70%, or 60,000–100,000 cells of DLD-1, SW480, RKO, or PaTu 8988 t were plated and transfected for 96 hours in 6-well plates. Eight hundred to 2000 of DLD-1, SW480, RKO, or PaTu 8988t cells were then transferred to 96-well plates to reach a final confluence of 50%-70% and allowed to adhere overnight before being treated with various drugs at multiple concentrations for 120 hours. Following incubation, the cells were washed and lysed in 100 µl H_2O, and 0.2% SYBR Green (Lonza, Cologne, Germany) was added. Fluorescence was measured using a Victor^3 V plate reader (PerkinElmer, Waltham, MA), and growth inhibition was calculated as compared to the untreated control samples.

Immunoblotting

Cells were lysed and protein extracts boiled and loaded on 10% or 15% polyacrylamide gels. After electrophoretic separation, the proteins were transferred to PVDF membranes, which were blocked with 5% milk powder in TBS + 0.1% Tween 20 (TBS-T) for 1 hour. Incubation of the primary antibody in TBS-T was performed at 4°C overnight. Membranes were then washed and stained with secondary antibody. Chemiluminescence was elicited using Western Lightning Ultra from PerkinElmer or Clarity Western ECL Substrate from Bio-Rad Laboratories (Munich, Germany), respectively, according to the manufacturers' instructions. The following primary antibodies were used: anti-Caspase 3, anti-cleaved Caspase 3 (Asp175), anti-Caspase 8 (1C12), anti-PARP, anti-pCHK1 (Ser345) (133D3), and anti-PRIM1 (8G10) from Cell Signaling Technology (Cambridge, UK); anti-ATR (N-19), anti-Caspase 9 (H-170), anti-Cdc25A (5H51), anti-CHK1 (G4), anti-Cyclin A (H-432), and anti-Wee1 (B-11) from Santa Cruz Biotechnology (Dallas, TX); and anti-β-Actin (AC-15) from Sigma-Aldrich. HRP-conjugated anti-goat, anti-rat, anti-mouse, and anti-rabbit antibodies from Santa Cruz Biotechnology were used as secondary antibodies.

γH2AX Immunofluorescence

Cells were seeded and transfected on coverslips in 6-well plates to reach a final confluence of 50%-70%. One hundred twenty hours later, cells were washed with phosphate-buffered saline (PBS) and fixed in 3.7% formaldehyde for 10 minutes. After a short incubation in ice-cold methanol, the cells were washed in PBS and then permeabilized in TBS + 0.5% Triton X-100 for 10 minutes and incubated in blocking solution (TBS + 0.5%Triton X-100 + 2% BSA) for 30 minutes. Primary antibody targeting γH2AX (20E3) (Cell Signaling Technology) was diluted in the blocking solution and applied at 4°C overnight. Cells were washed and incubated with the secondary antibody conjugated with Alexa Fluor 488 (Life Technologies, Carlsbad, CA) for 2 hours. Then, slides were washed

and mounted with Roti-Mount FluorCare (Carl Roth, Karlsruhe, Germany) containing DAPI. The Axiovert 200 M fluorescent microscope and the AxioVision Rel. 4.8 software (Carl Zeiss, Jena, Germany) were used for analysis. Exposure time and settings were kept constant for all samples within an individual experiment. Three independent experiments were performed, and for each cell line and condition, at least 70 cells were scored.

Cell Cycle Analysis

Cells were seeded and transfected in 6-well plates to reach a confluence of 50%-70% at the time of analysis. After 72-144 hours, cells were collected, washed, and stained with propidium iodide (0.1% sodium citrate, 0.1% Triton X-100, and 50 µg/ml propidium iodide) as described previously [15]. Cell cycle distribution was quantified by using the BD FACSCanto II from BD Biosciences (San Jose, CA) and the FlowJo v10 software from FlowJo, LLC (Ashland, OR). At least 20,000 gated events per sample were analyzed.

Statistical Analyses

All statistical analyses were performed using Prism 5 from GraphPad Software (La Jolla, CA). Error bars represent ±SEM of at least three independent experiments. Surviving fractions of the proliferation assays were calculated by curve fitting with nonlinear regression. A two-tailed, unpaired Student's *t* test was used for statistical interpretation; *P* values of $P < .05$ (*), $P < .01$ (**), or $P < .001$ (***) were considered statistically significant.

Results

Verification of Synthetic Lethality Between ATR and PRIM1

To exclude artifacts due to clonal variation, we extended our human CRC DLD-1 *ATR* knock-in model, consisting of parental *ATR*-proficient ($ATR^{+/+}$) and *ATR*-defective ($ATR^{s/s}$) cells, to *ATR* reexpressing cells (ATR^{resc}). ATR protein levels were quantified by immunoblotting (Figure 1*A*), confirming subtotal ATR protein depletion in $ATR^{s/s}$ and reexpression of ATR protein in ATR^{resc} cells. The increased sensitivity of $ATR^{s/s}$ cells towards the DNA interstrand-crosslinking (ICL) agent MMC [13] was partially reversible in ATR^{resc} cells (Figure 1*B*). Similarly, the previously reported [9] proliferation inhibition of $ATR^{s/s}$ cells upon siRNA-mediated *PRIM1* depletion (Figure 1*C*) was also partially reversible upon *ATR* reexpression (Figure 1*D*). Thus, the previously observed detrimental effects of *PRIM1* depletion on *ATR*-deficient cells are *ATR* specific, excluding clonal variation as a confounding variable.

siPRIM1-Mediated Sensitization of DLD-1 Cells to ATR and CHK1 Inhibitors

We next assessed whether the detrimental effects of *PRIM1* depletion on cells with genetic *ATR* defects were similarly inducible using chemical ATR inhibition in *ATR*-proficient DLD-1 cells. Therefore, *PRIM1*-depleted (Figure 2*A*), mock-, and nontransfected cells (NTC) were treated with the selective ATR inhibitors AZD6738 or VE-822 [16,17]. *PRIM1* depletion significantly increased the

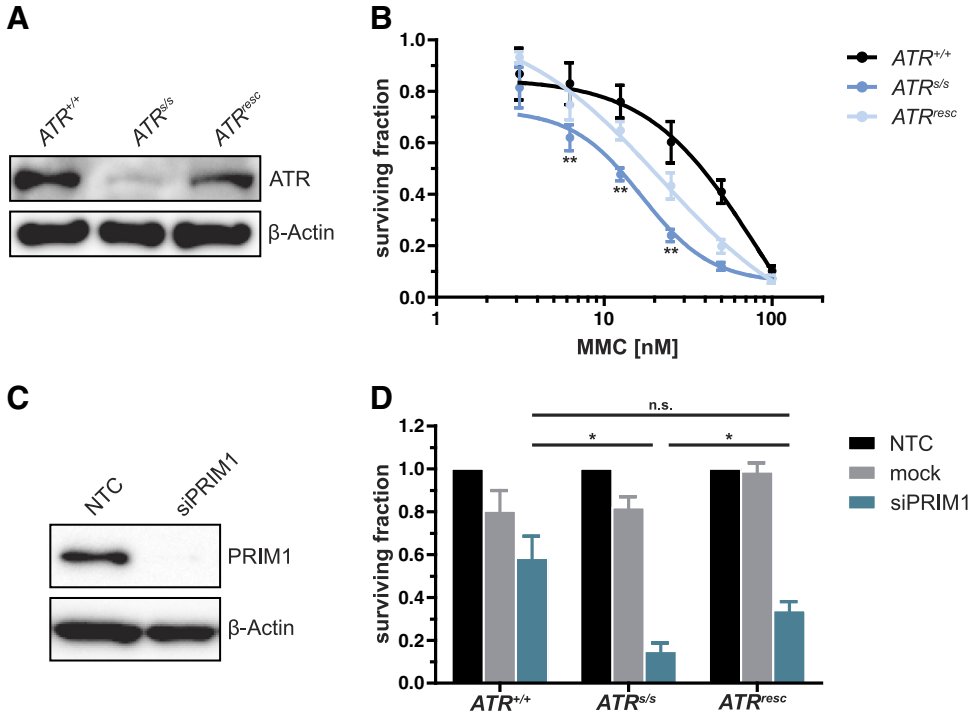

Figure 1. Verification of synthetic lethality between *ATR* and *PRIM1*. (A) Quantification of ATR protein in DLD-1 $ATR^{+/+}$, $ATR^{s/s}$, and ATR^{resc} cells by immunoblotting. β-Actin was used as loading control. (B) MMC sensitivity was assessed 120 hours after treatment by proliferation assay in DLD-1 $ATR^{+/+}$, $ATR^{s/s}$, and ATR^{resc} cells. (C) Quantification of siRNA-mediated *PRIM1* depletion (10 nM) 120 hours after transfection by immunoblotting. β-Actin was used as loading control. (D) Proliferation inhibition was assessed 144 hours after transfection by proliferation assay in DLD-1 $ATR^{+/+}$, $ATR^{s/s}$, and ATR^{resc} cells. Error bars represent ±SEM of three independent experiments with each data point reflecting triplicate wells. Asterisks mark statistical significance using a two-tailed, unpaired Student's *t* test (*$P < .05$, **$P < .01$, n.s. = not significant). Immunoblots were performed independently at least twice, and representative results are shown.

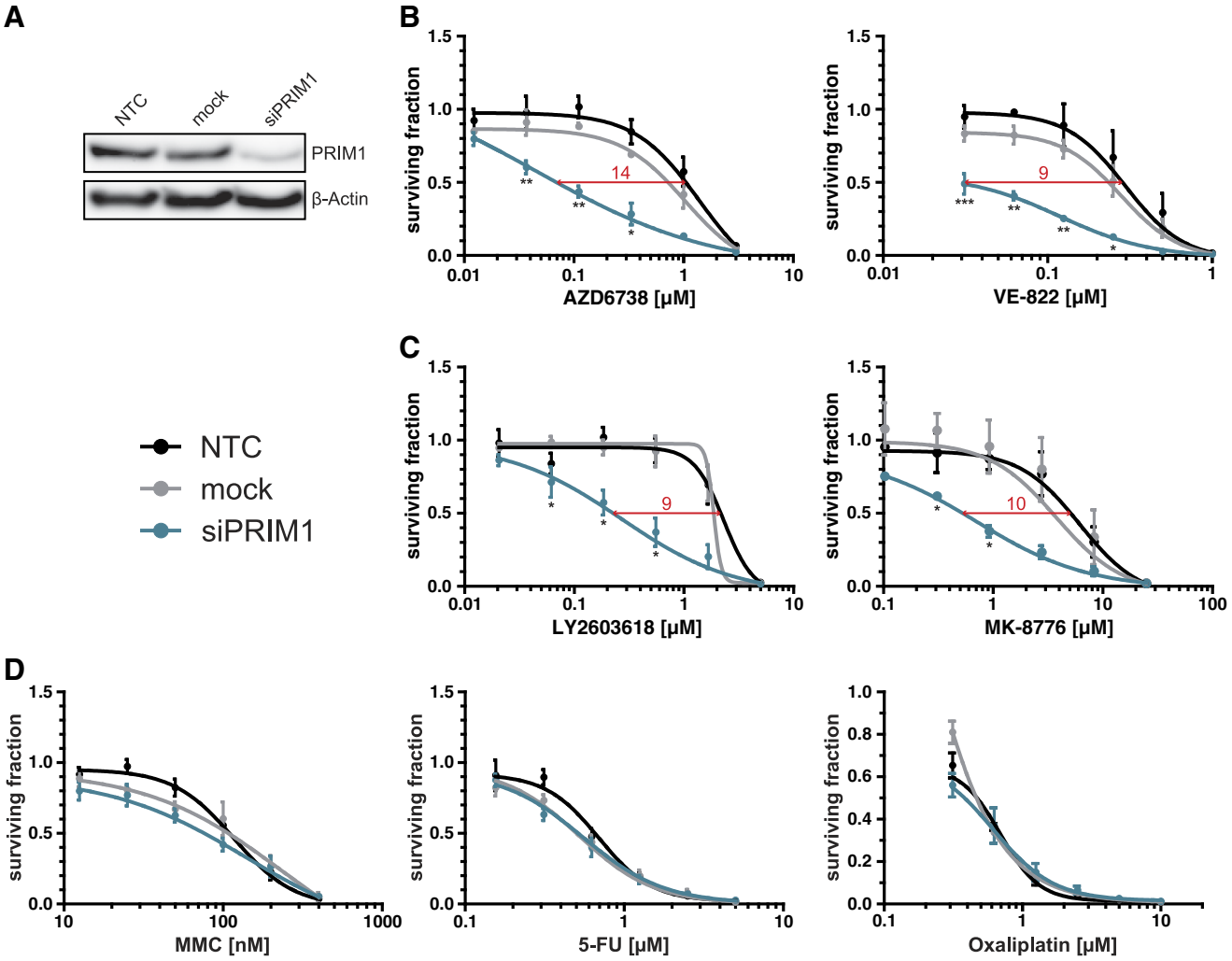

Figure 2. siPRIM1-mediated sensitization of DLD-1 cells to ATR and CHK1 inhibitors. (A) Knockdown efficiency of PRIM1 via siRNA was confirmed by immunoblotting 96 hours after transfection. β-Actin was used as loading control. (B) Effects of ATR inhibitors, (C) CHK1 inhibitors, and (D) common chemotherapeutics on the proliferation of *PRIM1*-depleted DLD-1 cells as compared to control and mock-transfected cells measured 120 hours after drug treatment. Error bars represent ±SEM of three independent experiments with each data point reflecting triplicate wells. Asterisks mark statistical significance using a two-tailed, unpaired Student's *t* test (*$P < .05$, **$P < .01$, ***$P < .001$). Immunoblots were performed independently at least three times, and representative results are shown.

sensitivity of DLD-1 cells to treatment with ATR inhibitors (IC_{50} ratios 14 and 9, respectively; Figure 2*B*). Similar effects were observed upon treatment with selective inhibitors of CHK1, the major downstream effector kinase of ATR, applying LY2603618 or MK-8776 [18–20] (IC_{50} ratios 9 and 10, respectively; Figure 2*C*).

To exclude a general and unspecific drug hypersensitivity upon *PRIM1* depletion, cells were additionally treated with common chemotherapeutics including MMC, 5-FU, and oxaliplatin. No significant *PRIM1*-dependent effects were observed (Figure 2*D*). Thus, *PRIM1* depletion sensitizes DLD-1 cells specifically to ATR and CHK1 inhibitors but not towards common chemotherapeutics.

siPRIM1-Mediated Sensitization to ATR and CHK1 Inhibitors in a Panel of Different Cancer Cell Lines

To generalize our data beyond one single cell line and to exclude confounding artifacts due to the microsatellite instability (MSI) phenotype of DLD-1 cells [21,22], we additionally analyzed the effects of ATR and CHK1 inhibitors upon *PRIM1* depletion on microsatellite-stable SW480 and microsatellite-instable RKO cells [21,22], both CRC cell lines, as well as on microsatellite-stable pancreatic cancer PaTu 8988t cells [23]. As demonstrated for DLD-1 cells, *PRIM1* depletion (Figure 3*A*) increased the sensitivity also of SW480, RKO, and PaTu 8988t cells to treatment with ATR inhibitors (IC_{50} ratios ranging from 4 to at least 13, Figure 3*B*) and CHK1 inhibitors (IC_{50} ratios ranging from 3 to at least 26, Figure 3*C*). Thus, siPRIM1-mediated sensitization to treatment with ATR and CHK1 inhibitors is independent of MSI status and applicable to multiple cell lines derived from different tumor entities.

siPRIM1-Mediated Effects on Cell Cycle Progression in $ATR^{s/s}$ Cells

To investigate the molecular mechanisms underlying the synthetic lethality between *ATR* and *PRIM1*, we compared the cell cycle profiles of $ATR^{+/+}$ versus $ATR^{s/s}$ cells upon *PRIM1* depletion. *ATR* deficiency of $ATR^{s/s}$ cells with consecutive loss of DNA damage checkpoint responses [24] expectedly resulted in a constitutively increased G_2/M fraction ($P < .001$) along with a slight but statistically nonsignificant ($P > .05$) decrease of the S-phase fraction (Figure 4*A*).

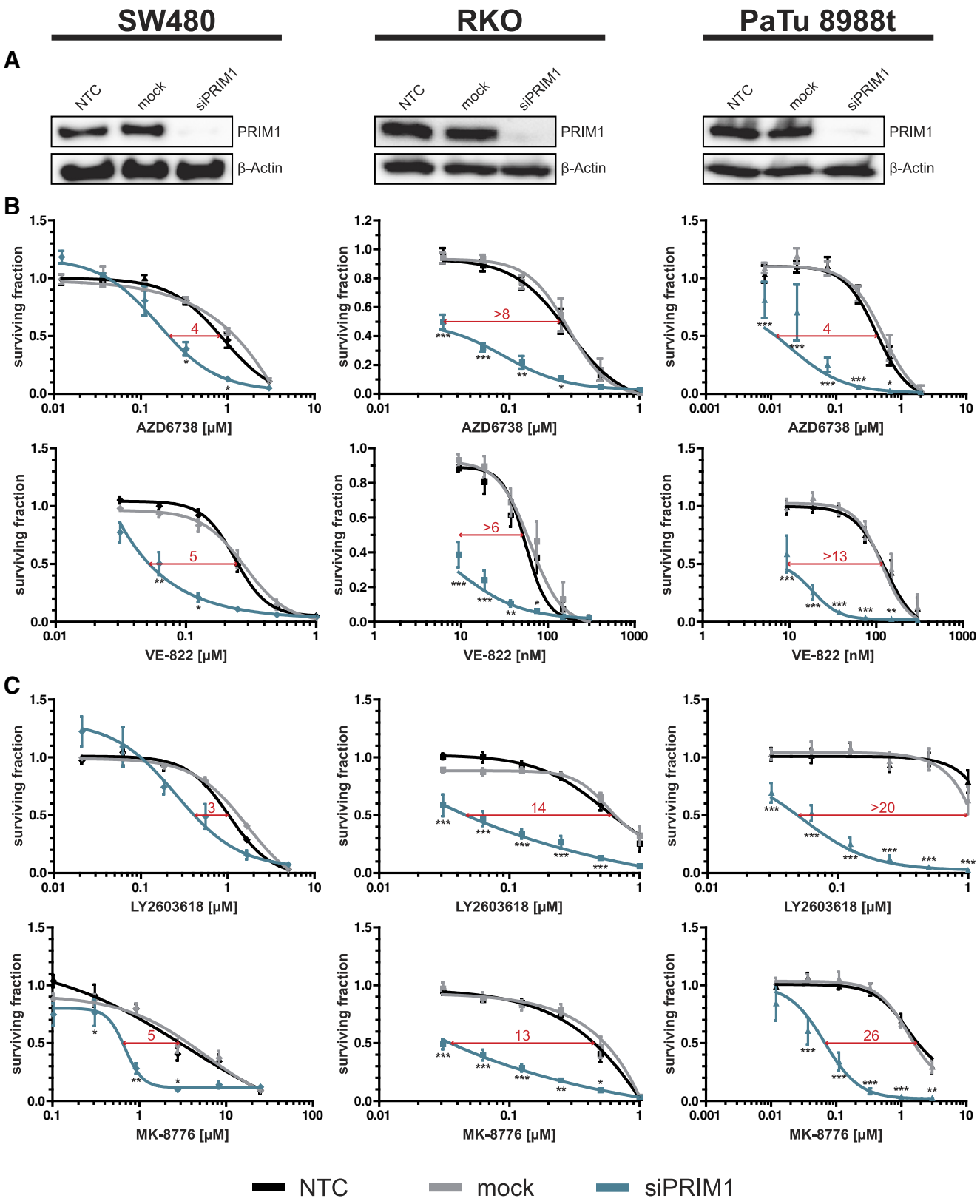

Figure 3. siPRIM1-mediated sensitization to ATR and CHK1 inhibitors in a panel of different cancer cell lines. (A) Knockdown efficiency of PRIM1 via siRNA was confirmed by immunoblotting 96 hours after transfection. β-Actin was used as loading control. (B) Effects of ATR and (C) CHK1 inhibitors on the proliferation of *PRIM1*-depleted SW480, RKO, and PaTu 8988t cells as compared to control and mock-transfected cells measured 120 hours after drug treatment. Error bars represent ±SEM of at least three independent experiments with each data point reflecting triplicate wells. Asterisks mark statistical significance using a two-tailed, unpaired Student's *t* test (*$P < .05$, **$P < .01$, ***$P < .001$). Immunoblots were performed independently at least three times, and representative results are shown.

Interestingly however, additional depletion of *PRIM1* caused a significant increase of the S-phase fraction specifically in $ATR^{s/s}$ cells (Figure 4*B*). To identify the mediators responsible for this effect, we quantified the cell cycle protein levels of CHK1, ATR's main effector kinase; Wee1, a key regulator of the cell cycle progression [25,26]; as well as Cdc25A and Cyclin A, representing mediators of G_1/S progression (Figure 4, *C* and *D*). Upon *PRIM1* depletion, CHK1 protein was activated through phosphorylation in an ATR-independent manner, the latter being consistent with a previous report of sufficient CHK1 phosphorylation in $ATR^{s/s}$ cells [10]. Furthermore, the kinase Wee1 was also regulated in a *PRIM1*-dependent fashion, i.e., upregulated in $ATR^{+/+}$ cells but downregulated in $ATR^{s/s}$ cells upon *PRIM1* depletion. Similarly, the phosphatase Cdc25A was upregulated in $ATR^{+/+}$ cells but downregulated in $ATR^{s/s}$ cells. Cyclin A appeared slightly upregulated in $ATR^{s/s}$ cells, but this effect did not reach statistical significance. Thus, the detrimental effects of *PRIM1* depletion on $ATR^{s/s}$ cells are at least in part attributable to S-phase impairment and concomitant downregulation of Wee1.

siPRIM1-Mediated Induction of Apoptosis on $ATR^{s/s}$ Cells

As *PRIM1* depletion significantly increased the sub-G_1 fraction specifically in $ATR^{s/s}$ cells (Figures 4*A* and 5*A*), we next quantified the protein levels of the central mediators of apoptosis in this context (Figure 5*B*). Only *PRIM1*-depleted *ATR*-deficient cells displayed cleavage of caspase 3 ($P < .05$), the main effector protease of apoptosis, along with cleavage of its substrate PARP ($P < .05$). Furthermore, we observed *PRIM1*-dependent cleavage of caspase 8 in $ATR^{s/s}$ cells ($P < .05$), indicating extrinsic apoptosis. Caspase 9 cleavage appeared to be independent of *PRIM1* status ($P > .05$).

To test whether apoptosis was attributable to the accumulation of DNA damage, we quantified the formation of γH2AX foci, which serve as surrogate marker for DNA double-strand breaks (DSBs) [27] (Figure 5*C*). $ATR^{s/s}$ cells expectedly displayed a slight but statistically not significant increase of γH2AX foci as compared to $ATR^{+/+}$ cells. This increase, however, was not augmented upon *PRIM1* depletion. Thus, the simultaneous depletion of *ATR* and *PRIM1* activates the extrinsic apoptosis pathway through cleavage of caspase 8 followed by cleavage of caspase 3 and PARP without evidence of increased accumulation of DNA damage.

Discussion

The principle of synthetic lethality offers new approaches for an individualized and targeted cancer therapy with reduced side effects [1]. In a previous study, we identified six DNA repair genes to act synthetically lethal with *ATR* by screening of an siRNA library directed against 288 DNA repair genes [9]. One of the identified genes was *PRIM1*, encoding for the catalytic subunit of primase, which is complexed with polymerase α. Together with polδ and polϵ, this polα-primase complex is crucial for DNA replication [11,12,28].

In this study, we used the CRC cell line DLD-1 homozygously harboring the hypomorphic *ATR* "Seckel" mutation A2101G [29], which results in a subtotal ATR protein depletion with an increased sensitivity to DNA-ICL agents but no significant effect on cell growth or viability [7,10,13,30]. This model was ideally suited for our

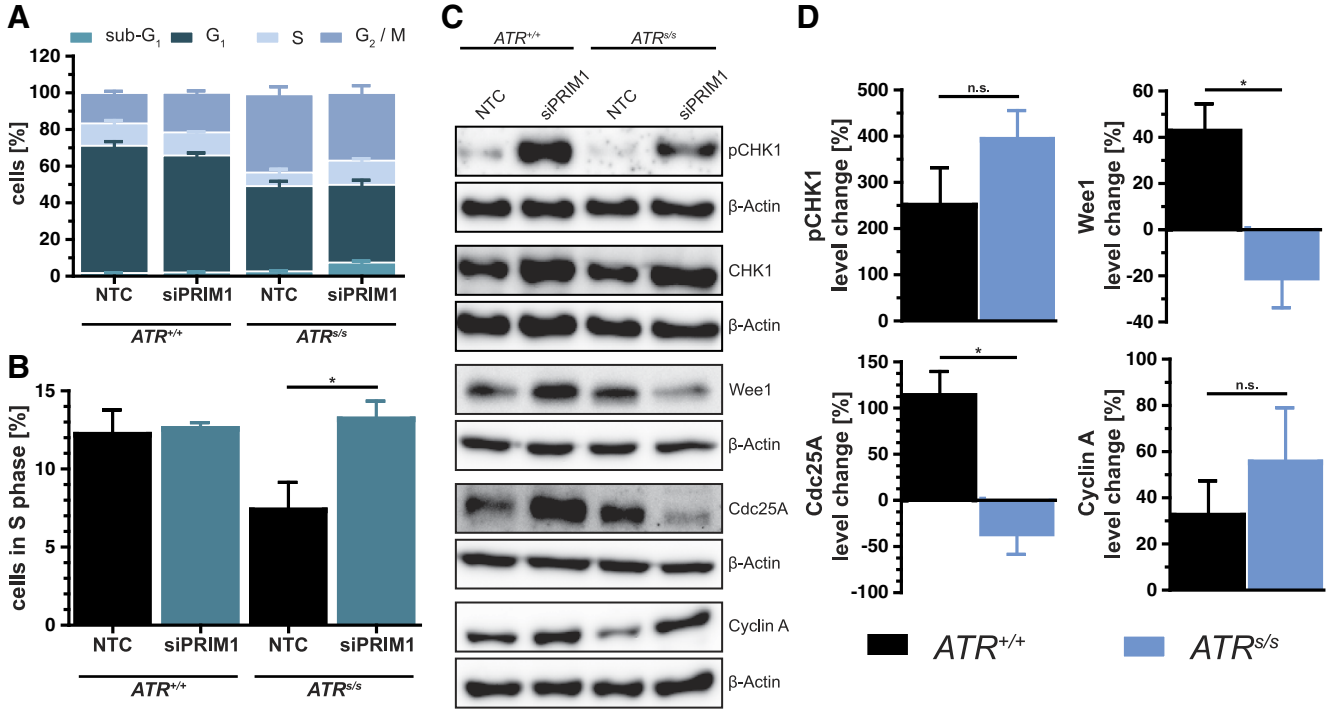

Figure 4. siPRIM1-mediated effects on cell cycle progression in $ATR^{s/s}$ cells. (A) Cell cycle profile of DLD-1 $ATR^{+/+}$ and $ATR^{s/s}$ cells 144 hours after siPRIM1 transfection as assessed by FACS analysis. (B) S-phase fraction of the cell cycle profile in detail. (C and D) Protein quantification in DLD-1 $ATR^{+/+}$ and $ATR^{s/s}$ cells by immunoblotting 144 hours after siPRIM1 transfection. β-Actin was used as loading control. Percentage protein change of *PRIM1*-depleted cells was normalized to NTC of DLD-1 $ATR^{+/+}$ and $ATR^{s/s}$ cells. Error bars represent ±SEM of three independent experiments. Asterisks mark statistical significance using a two-tailed, unpaired Student's *t* test (*$P < .05$, n.s. = not significant). Immunoblots were performed independently at least three times, and representative results are shown.

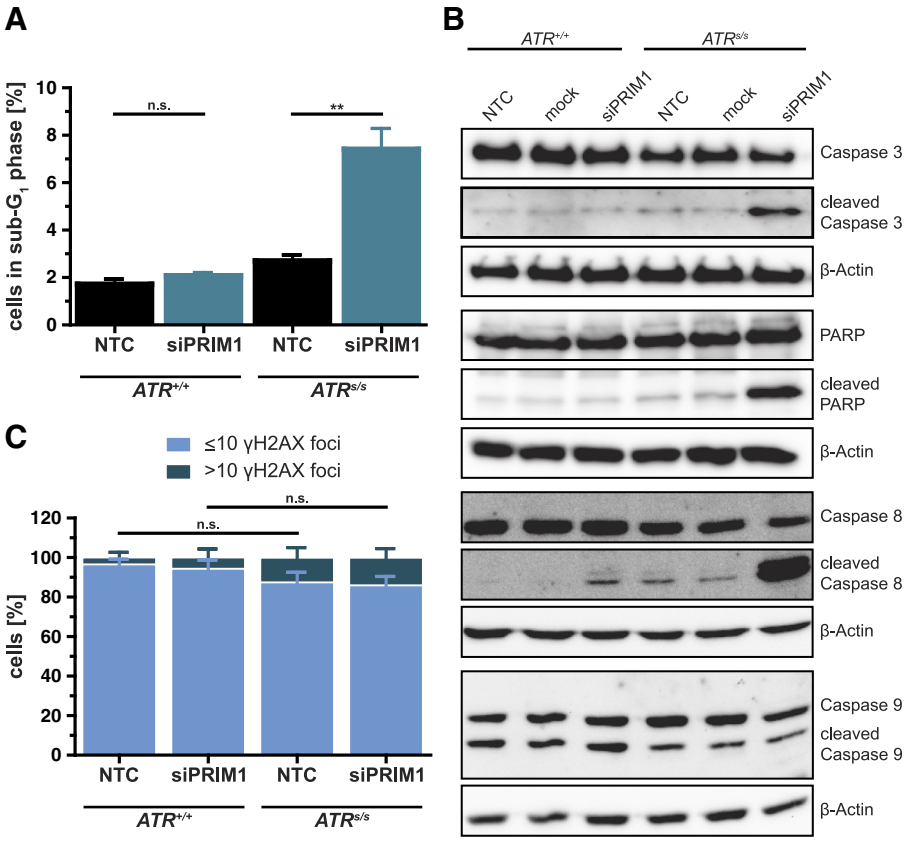

Figure 5. siPRIM1-mediated induction of apoptosis on *ATR*$^{s/s}$ cells. (A) Sub-G_1 fraction from the cell cycle profile (Figure 4*A*) in detail. (B) Cleavage of PARP and caspase 3, 8, and 9 in DLD-1 *ATR*$^{+/+}$ and *ATR*$^{s/s}$ cells was assessed by immunoblotting 144 hours after siPRIM1 transfection. β-Actin was used as loading control. (C) γH2AX quantification in DLD-1 *ATR*$^{+/+}$ and *ATR*$^{s/s}$ cells 120 hours after siPRIM1 transfection. Error bars represent ±SEM of three independent experiments. Asterisks mark statistical significance using a two-tailed, unpaired Student's *t* test (**$P < .01$, n.s. = not significant). Immunoblots were performed independently at least twice, and representative results are shown.

experiments, as the subtotal ATR protein depletion mimics the incomplete pharmacological ATR inhibition more closely than a complete and in most instances lethal *ATR* gene knockout [24]. First, we confirmed the synthetic lethality between *ATR* and *PRIM1* by demonstrating proliferation inhibition of *ATR*$^{s/s}$ cells upon *PRIM1* depletion. To exclude clonal variation as a confounding artifact, we additionally established a rescue cell clone, which demonstrated that these effects were reversible upon ATR reexpression.

Based on these data, we asked whether these detrimental effects on *ATR*-deficient cells upon *PRIM1* depletion could also be elicited in *ATR*-proficient cells by using ATR pathway-inhibiting chemical agents, i.e., clinically relevant ATR inhibitors or inhibitors, towards its main effector kinase CHK1 [18–20]. In fact, both ATR and CHK1 inhibitors decreased proliferation of *PRIM1*-depleted DLD-1 cells, suggesting PRIM1 inactivation as a potential predictive biomarker for sensitivity to these agents. Importantly, we were able to show similar results in a panel of cancer cell lines, including SW480, RKO, and PaTu 8988t, suggesting these effects to be independent of MSI status and generalizable to different tumor types.

Mechanistically, *PRIM1* depletion increased the S-phase fraction in *ATR*$^{s/s}$ cells. Concomitant downregulation of Cdc25A indicated a cell cycle arrest in S-phase [31]. However, the virtually undiminished Cyclin A protein levels in *PRIM1*-depleted *ATR*$^{s/s}$ cells suggested S-phase stasis rather than a classical S-phase arrest [32]. Consistently, Hurley and colleagues described that ionizing radiation of *ATR*$^{s/s}$ cells leads to a prolonged S-phase that closely resembled S-phase stasis [10]. Taken together with the concomitant CHK1 activation observed in our experiments, S-phase stasis induced by *PRIM1* depletion in *ATR*$^{s/s}$ cells might represent an unresolvable replication catastrophe.

Perhaps even more importantly, apoptosis contributed to the *PRIM1*-dependent inhibition of proliferation, as shown by the increased sub-G_1 fraction in *PRIM1*-depleted *ATR*$^{s/s}$ cells along with cleavage of the common apoptosis effector enzymes PARP and caspase 3. Surprisingly, the additional cleavage of caspase 8 points towards extrinsic apoptosis, which is predominantly mediated by death receptors, rather than intrinsic apoptosis [33]. This effect could be mechanistically attributable to the concomitant downregulation of Wee1 in *ATR*$^{s/s}$ cells upon *PRIM1* depletion, which leads to apoptosis [34] through upregulation of death receptors [35] and might thus represent a protective cellular response to replication catastrophe. Interestingly, apoptosis appeared not to be attributable to the increased formation of DSBs.

From a clinical-translational perspective, germline mutations in *POLD1* and *POLE*, the catalytic subunits of polδ and polϵ, were recently reported in colorectal and other cancers [36–38]. In contrast, little is known about the prevalence of genetic alterations of *PRIM1* or other components of the polα-primase complex in cancer: the

amplification of a large region including the *PRIM1* gene locus was reported in osteosarcoma [39], and upregulation of *PRIM1* gene expression was reported in lung cancer [40] and breast cancer [41]. According to the Catalogue Of Somatic Mutations In Cancer, less than 1% of tested tumor samples show mutations in *PRIM1* or the three other subunits of the polα-primase complex: *PRIM2*, *POLA1*, and *POLA2* [42]. Nevertheless, the exact prevalence of mutations in the polα-primase complex should be evaluated systematically in different tumor types. Vice versa, testing the effects of inhibition of any component of this polα-primase complex on *ATR*-deficient cancer cells could clarify whether *ATR* deficiency in cancer might be therapeutically targetable by any type of inhibition of the polα-primase complex. In fact, preliminary experiments from our lab suggest that $ATR^{s/s}$ cells exhibit increased sensitivity to ST1926 (unpublished observations), a compound recently shown to inhibit polymerase α in colorectal cancer cells [43–45].

Conclusions

We demonstrated that *PRIM1* inactivation sensitizes cancer cells to ATR and CHK1 inhibitors via S-phase stasis and Wee1-mediated, caspase 8–dependent apoptosis. Hence, mutations in *PRIM1* or other components of the polα-primase complex could represent novel targets for individualized tumor therapeutic approaches using ATR or CHK1 inhibitors, as has similarly been proposed for *POLD1* [9]. Vice versa, cancer cells naturally harboring inactivating *ATR* (or *CHK1*) mutations might exhibit increased sensitivity to inhibitors targeting any component of the polα-primase complex.

Acknowledgements

We thank Bettina Geisel for expert technical assistance. This work was funded in part by a grant of Deutsche Forschungsgemeinschaft to E. G. (DFG 762/3-2) and by the European Union's Seventh Framework Programme to T. M. G. (EU FP7 602783, "CAM-PaC"). This paper reflects only the authors' views, and the European Union is not liable for any use that may be made of the information contained therein.

Availability of Data and Material

The datasets used and/or analyzed during the current study are available from the corresponding author on reasonable request.

Authors' Contribution

A. J. designed, performed, and analyzed the experiments and drafted the manuscript. L.-M. S., L. v. W., and B. L. B. performed some experiments. T. M. G. and M. B. provided important intellectual content. E. G. designed, analyzed, and supervised the study and wrote the final manuscript. All authors read and approved the final manuscript. These data are part of A. J.'s doctoral thesis.

References

[1] Kaelin WG (2005). The concept of synthetic lethality in the context of anticancer therapy. *Nat Rev Cancer* **5**(9), 689–698.

[2] Scott CL, Swisher EM, and Kaufmann SH (2015). Poly (ADP-ribose) polymerase inhibitors: recent advances and future development. *J Clin Oncol* **33**(12), 1397–1406.

[3] Sonnenblick A, de Azambuja E, Azim HA, and Piccart M (2015). An update on PARP inhibitors–moving to the adjuvant setting. *Nat Rev Clin Oncol* **12**(1), 27–41.

[4] Paulsen RD and Cimprich KA (2007). The ATR pathway: fine-tuning the fork. *DNA Repair* **6**(7), 953–966.

[5] Cimprich KA and Cortez D (2008). ATR: an essential regulator of genome integrity. *Nat Rev Mol Cell Biol* **9**(8), 616–627.

[6] Zhou BB and Elledge SJ (2000). The DNA damage response: putting checkpoints in perspective. *Nature* **408**(6811), 433–439.

[7] Gallmeier E, Hermann PC, Mueller M-T, Machado JG, Ziesch A, De Toni EN, Palagyi A, Eisen C, Ellwart JW, and Rivera J, et al (2011). Inhibition of ataxia telangiectasia- and Rad3-related function abrogates the in vitro and in vivo tumorigenicity of human colon cancer cells through depletion of the CD133(+) tumor-initiating cell fraction. *Stem Cells* **29**(3), 418–429. https://doi.org/10.1002/stem.595 [URL http://www.ncbi.nlm.nih.gov/pubmed/21308861].

[8] Wagner JM and Kaufmann SH (2010). Prospects for the use of ATR inhibitors to treat cancer. *Pharmaceuticals* **3**(5), 1311–1334. https://doi.org/10.3390/ph3051311 [URL http://www.ncbi.nlm.nih.gov/pubmed/27713304, http://www.pubmedcentral.nih.gov/articlerender.fcgi?artid=PMC4033983].

[9] Hocke S, Guo Y, Job A, Orth M, Ziesch A, Lauber K, De Toni EN, Gress TM, Herbst A, and Göke B, et al (2016). A synthetic lethal screen identifies ATR-inhibition as a novel therapeutic approach for POLD1-deficient cancers. *Oncotarget* **7**(6), 7080–7095.

[10] Hurley PJ, Wilsker D, and Bunz F (2007). Human cancer cells require ATR for cell cycle progression following exposure to ionizing radiation. *Oncogene* **26**(18), 2535–2542.

[11] Copeland WC and Wang TS (1993). Enzymatic characterization of the individual mammalian primase subunits reveals a biphasic mechanism for initiation of DNA replication. *J Biol Chem* **268**(35), 26179–26189.

[12] Waga S and Stillman B (1998). The DNA replication fork in eukaryotic cells. *Annu Rev Biochem* **67**(1), 721–751.

[13] Gallmeier E, Hucl T, Calhoun ES, Cunningham SC, Bunz F, Brody JR, and Kern SE (2007). Gene-specific selection against experimental fanconi anemia gene inactivation in human cancer. *Cancer Biol Ther* **6**(5), 654–660.

[14] Jiang G and Sancar A (2006). Recruitment of DNA damage checkpoint proteins to damage in transcribed and nontranscribed sequences. *Mol Cell Biol* **26**(1), 39–49.

[15] Nicoletti I, Migliorati G, Pagliacci MC, Grignani F, and Riccardi C (1991). A rapid and simple method for measuring thymocyte apoptosis by propidium iodide staining and flow cytometry. *J Immunol Methods* **139**(2), 271–279.

[16] Pihlak R, Valle JW, and McNamara MG (2017). Germline mutations in pancreatic cancer and potential new therapeutic options. *Oncotarget* **8**(42), 73240–73257.

[17] Karnitz LM and Zou L (2015). Molecular pathways: targeting ATR in cancer therapy. *Clin Cancer Res* **21**(21), 4780–4785.

[18] Scagliotti G, Kang JH, Smith D, Rosenberg R, Park K, Kim S-W, Su W-C, Boyd TE, Richards DA, and Novello S, et al (2016). Phase II evaluation of LY2603618, a first-generation CHK1 inhibitor, in combination with pemetrexed in patients with advanced or metastatic non–small cell lung cancer. *Invest New Drugs* **34**(5), 625–635.

[19] Daud AI, Ashworth MT, Strosberg J, Goldman JW, Mendelson D, Springett G, Venook AP, Loechner S, Rosen LS, and Shanahan F, et al (2015). Phase I dose-escalation trial of checkpoint kinase 1 inhibitor MK-8776 as monotherapy and in combination with gemcitabine in patients with advanced solid tumors. *J Clin Oncol* **33**(9), 1060–1066.

[20] Webster JA, Tibes R, Morris L, Blackford AL, Litzow M, Patnaik M, Rosner GL, Gojo I, Kinders R, and Wang L, et al (2017). Randomized phase II trial of cytosine arabinoside with and without the CHK1 inhibitor MK-8776 in relapsed and refractory acute myeloid leukemia. *Leuk Res* **61**, 108–116.

[21] Ahmed D, Eide PW, Eilertsen IA, Danielsen SA, Eknæs M, Hektoen M, Lind GE, and Lothe RA (2013). Epigenetic and genetic features of 24 colon cancer cell lines. *Oncogene* **2**(9), e71.

[22] Ku JL, Yoon KA, Kim DY, and Park JG (1999). Mutations in hMSH6 alone are not sufficient to cause the microsatellite instability in colorectal cancer cell lines. *Eur J Cancer* **35**(12), 1724–1729 [URL http://www.ncbi.nlm.nih.gov/pubmed/10674020].

[23] Elsässer HP, Lehr U, Agricola B, and Kern HF (1992). Establishment and characterisation of two cell lines with different grade of differentiation derived from one primary human pancreatic adenocarcinoma. *Virchows Arch B Cell Pathol Incl Mol Pathol* **61**(5), 295–306 [URL http://www.ncbi.nlm.nih.gov/pubmed/1348891].

[24] Cortez D, Guntuku S, Qin J, and Elledge SJ (2001). ATR and ATRIP: partners in checkpoint signaling. *Science* **294**(5547), 1713–1716.

[25] Do K, Doroshow JH, and Kummar S (2013). Wee1 kinase as a target for cancer therapy. *Cell Cycle* **12**(19), 3159–3164.

[26] Matheson CJ, Backos DS, and Reigan P (2016). Targeting WEE1 kinase in cancer. *Trends Pharmacol Sci* **37**(10), 872–881.

[27] Rogakou EP, Pilch DR, Orr AH, Ivanova VS, and Bonner WM (1998). DNA double-stranded breaks induce histone H2AX phosphorylation on serine 139. *J Biol Chem* **273**(10), 5858–5868.
[28] Pellegrini L (2012). The Pol α-primase complex. *Subcell Biochem* **62**, 157–169.
[29] O'Driscoll M, Ruiz-Perez VL, Woods CG, Jeggo PA, and Goodship JA (2003). A splicing mutation affecting expression of ataxia-telangiectasia and Rad3-related protein (ATR) results in Seckel syndrome. *Nat Genet* **33**(4), 497–501.
[30] Wilsker D and Bunz F (2007). Loss of ataxia telangiectasia mutated- and Rad3-related function potentiates the effects of chemotherapeutic drugs on cancer cell survival. *Mol Cancer Ther* **6**(4), 1406–1413.
[31] Molinari M, Mercurio C, Dominguez J, Goubin F, and Draetta GF (2000). Human Cdc25 A inactivation in response to S phase inhibition and its role in preventing premature mitosis. *EMBO Rep* **1**(1), 71–79.
[32] Borel F, Lacroix FB, and Margolis RL (2002). Prolonged arrest of mammalian cells at the G1/S boundary results in permanent S phase stasis. *J Cell Sci* **115**(Pt 14), 2829–2838.
[33] Chen M and Wang J (2002). Initiator caspases in apoptosis signaling pathways. *Apoptosis* **7**(4), 313–319.
[34] Tominaga Y, Li C, Wang R-H, and Deng C-X (2006). Murine Wee1 plays a critical role in cell cycle regulation and pre-implantation stages of embryonic development. *Int J Biol Sci* **2**(4), 161–170.
[35] Garimella SV, Rocca A, and Lipkowitz S (2012). WEE1 inhibition sensitizes basal breast cancer cells to TRAIL-induced apoptosis. *Mol Cancer Res* **10**(1), 75–85.
[36] Bellido F, Pineda M, Aiza G, Valdés-Mas R, Navarro M, Puente DA, Pons T, González S, Iglesias S, and Darder E, et al (2016). POLE and POLD1 mutations in 529 kindred with familial colorectal cancer and/or polyposis: review of reported cases and recommendations for genetic testing and surveillance. *Genet Med* **18**(4), 325–332.
[37] Palles C, Cazier J-B, Howarth KM, Domingo E, Jones AM, Broderick P, Kemp Z, Spain SL, Guarino E, and Guarino Almeida E, et al (2013). Germline mutations affecting the proofreading domains of POLE and POLD1 predispose to colorectal adenomas and carcinomas. *Nat Genet* **45**(2), 136–144 [URL http://www.ncbi.nlm.nih.gov/pubmed/23263490, http://www.pubmedcentral.nih.gov/articlerender.fcgi?artid=PMC3785128].
[38] Valle L, Hernández-Illán E, Bellido F, Aiza G, Castillejo A, Castillejo M-I, Navarro M, Seguí N, Vargas G, and Guarinos C, et al (2014). New insights into POLE and POLD1 germline mutations in familial colorectal cancer and polyposis. *Hum Mol Genet* **23**(13), 3506–3512 [URL http://www.ncbi.nlm.nih.gov/pubmed/24501277].
[39] Yotov WV, Hamel H, Rivard GE, Champagne MA, Russo PA, Leclerc JM, Bernstein ML, and Levy E (1999). Amplifications of DNA primase 1 (PRIM1) in human osteosarcoma. *Genes Chromosomes Cancer* **26**(1), 62–69.
[40] Xu H, Ma J, Wu J, Chen L, Sun F, Qu C, Zheng D, and Xu S (2016). Gene expression profiling analysis of lung adenocarcinoma. *Braz J Med Biol Res* **49**(3) e4861.
[41] Lee W-H, Chen L-C, Lee C-J, Huang C-C, Ho Y-S, Yang P-S, Ho C-T, Chang H-L, Lin I-H, Chang H-W, Liu Y-R, Wu C-H, and Tu S-H (2018). DNA primase polypeptide 1 (PRIM1) involves in estrogen-induced breast cancer formation through activation of the G2/M cell cycle checkpoint. *Int J Cancer* . https://doi.org/10.1002/ijc.31788 [URL http://www.ncbi.nlm.nih.gov/pubmed/30097999].
[42] COSMIC, Sanger Institute's Catalogue Of Somatic Mutations In Cancer. Retrieved from http://cancer.sanger.ac.uk/cosmic; 2018, Accessed date: 5 February 2018 . [URL http://cancer.sanger.ac.uk/cosmic].
[43] Garattini E, Parrella E, Diomede L, Gianni' M, Kalac Y, Merlini L, Simoni D, Zanier R, Ferrara FF, and Chiarucci I, et al (2004). ST1926, a novel and orally active retinoid-related molecule inducing apoptosis in myeloid leukemia cells: modulation of intracellular calcium homeostasis. *Blood* **103**(1), 194–207. https://doi.org/10.1182/blood-2003-05-1577 [URL http://www.ncbi.nlm.nih.gov/pubmed/12958071].
[44] Han T, Goralski M, Capota E, Padrick SB, Kim J, Xie Y, and Nijhawan D (2016). The antitumor toxin CD437 is a direct inhibitor of DNA polymerase α. *Nat Chem Biol* **12**(7), 511–515. https://doi.org/10.1038/nchembio.2082 [URL http://www.ncbi.nlm.nih.gov/pubmed/25246403, http://www.pubmedcentral.nih.gov/articlerender.fcgi?artid=PMC4249520, http://www.ncbi.nlm.nih.gov/pubmed/27182663, http://www.pubmedcentral.nih.gov/articlerender.fcgi?artid=PMC4912453].
[45] Abdel-Samad R, Aouad P, Gali-Muhtasib H, Sweidan Z, Hmadi R, Kadara H, D'Andrea EL, Fucci A, Pisano C, and Darwiche N (2018). Mechanism of action of the atypical retinoid ST1926 in colorectal cancer: DNA damage and DNA polymerase α. *Am J Cancer Res* **8**(1), 39–55.